The EUV Program at ASML: an update

Hans Meiling, Vadim Banine, Peter Kürz[a], Brian Blum[b], Gert Jan Heerens[c], and Noreen Harned[b]

ASML, P.O. Box 324, 5500 AH Veldhoven, The Netherlands
[a]Carl Zeiss, 73446 Oberkochen, Germany
[b]ASML, 77 Danbury Road, Wilton, CT 06897, USA
[c]TNO TPD, Stieltjesweg 1, 2600 AD Delft, The Netherlands

ABSTRACT

With the realisation of the α-tool, ASML is progressing with the pre-commercialisation phase of its EUVL development. We report on the progress in the development of several key modules of the α-tool, including the source, wafer stage and reticle stage, wafer handling, baseframe, and optics modules. We demonstrate that the focus sensor meets its vacuum requirements, and that both stages after limited servo optimisation approach the required scanning performance. A particle detection system has been build for the qualification of the reticle handling module, and preliminary results show that 50nm particles can be detected. The optics lifetime program showed substantial progress by utilising caplayers to MoSi samples in order to suppress oxidation caused by H_2O molecules under EUV illumination: a suppression $\geq$100× is achieved, compared to uncapped MoSi.

1. INTRODUCTION

The challenges we face in moving extreme ultraviolet lithography (EUVL) technology to commercialization are still significant, though progress has been made in all areas over the past year. Key areas of concern for EUVL are still

- high powered source of clean photons,
- optics that have "perfect" surfaces to support sub-50nm imaging,
- reticle transport and handling without the benefit of a pellicle,
- vacuum technology
- high sensitivity resist development with low line edge roughness.

We have moved well into feasibility in most of these critical areas, and are focusing on pushing to higher levels of performance with the targets for commercialization in mind. E.g., we need to investigate alternatives to get enough power so that EUV tools can achieve >100 wph. Also, we want the optics to survive 10 years at peak use. Reticles need to be particle free, but the industry wants the infrastructure to be as similar as possible to that for DUV. And vacuum technology – how will we translate this all to volume production?

ASML and Zeiss have continued to invest in developing answers to these challenges, even though the insertion of EUV for high volume production appears to be shifting to below the 50nm node. Key to our efforts is the design and realization of an Alpha tool (α-tool) [1] that helps to focus our efforts and enables risk reduction for commercialization. For the α-tool we have put the majority of the effort into those items that are unique to EUV, and for others have optimized for vacuum use of modules from our existing products. In this paper, we report on the progress of the α-tool development, focusing on these high risk items and progress as we bring the hardware to realization.

Emerging Lithographic Technologies VII, Roxann L. Engelstad, Editor,
Proceedings of SPIE Vol. 5037 (2003) © 2003 SPIE · 0277-786X/03/$15.00

2. SYSTEM DEVELOPMENT

In this section we will describe the progress in general system design, with emphasis on the source, wafer stage and reticle stage performance, and wafer handling.

2.1. Source development

The source is one of the highest risk items to the success of EUVL. Most EUV source developers use Xe in various forms (gaseous, frozen, droplets) as the target material. Although none of the currently known source concepts have demonstrated performance that would be compliant with the requirements for a high throughput EUVL production tool (115 W collected in-band EUV at intermediate focus for >100 300mm wph), significant progress has been reported and improvements in the future seems feasible. In Figure 1 we have compiled recently published data, which was presented both at the EUV Lithography Source workshop, in February 2002, and at the 1st International EUV Lithography Symposium (Oct. 2002). Several suppliers claim that in order to meet the high EUV power level needed for high throughput, non-Xe target material is essential due to the relatively low conversion efficiency of Xe of $\leq 1\%$ [2].

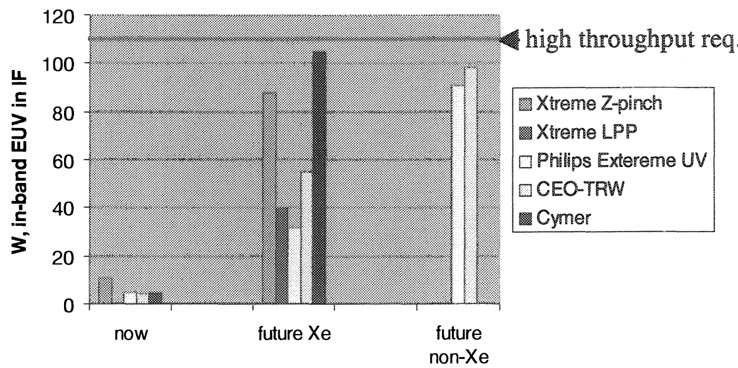

Figure 1. Status and predictions for in-band EUV power for various commercial suppliers of sources [2]. The red line denotes the target 115W in-band EUV power for production tools.

ASML addresses the critical item of the high power clean source in various ways. Specifications for a high power source required for a commercial EUV system are being set jointly with Nikon and Canon. Internal and external research is conducted to probe the fundamental limits of discharge sources, and to explore novel and alternative source target solutions. For a 100 wph commercial tool more than 115 Watt captured in-band clean photons are required [3]. The performance of the α-tool source will be evaluated on debris mitigation, vacuum concepts, and stability to the maximum power that can be provided, eventhough the 115-Watt power level obviously is not required for the α-tool. Throughput on the α-tool is in practice limited by the wafer handler and other non-EUV specific factors that will be redesigned for production tools.

As reported earlier [4] in the ASML EUV laboratory in Veldhoven, The Netherlands, an early prototype of the Philips hollow cathode discharge plasma source was installed in an experimental setup, see Figure 2. This source emits roughly 0.2 W in-band EUV at the intermediate focus of the source and condensor, and the concept of this EUV source was described by Bergman *et al.* [5].

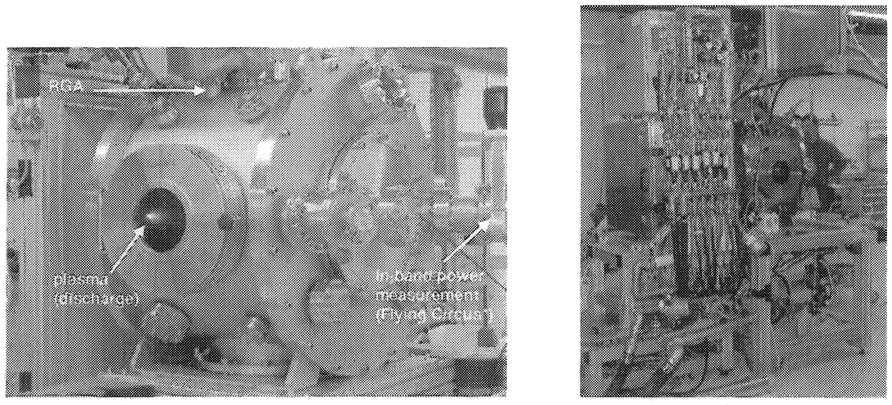

Figure 2. Progress in the HCT source development: on the left the 0.2 W experimental source that was installed in our EUV lab's test setup in 2001 [4], on the right the recently installed 5W source (2002).

In the framework of a joint research project between ASML and the Technical University of Eindhoven, theoretical and modeling efforts and fast EUV imaging and fast spectroscopy on this source are being combined, to further the knowledge on the dynamics of the EUV plasma pulse. The left-hand side images in Figure 3 show the time-resolved pinching process of the Xe-plasma, as registered with the pinhole camera. The time lapse between each picture is 5 ns. On the right-hand side in Figure 3 the emitted broad-band (10–18 nm) EUV spectrum is shown.

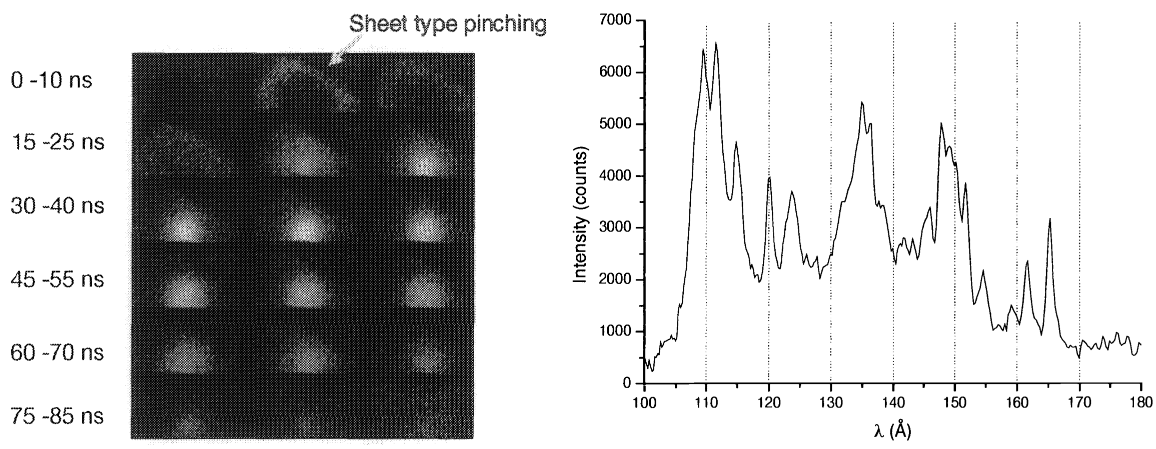

Figure 3. Time-resolved pinch images (left) and resulting broad-band EUV spectrum (right).

The conversion efficiency CE has been measured with a tool similar to the Flying Circus equipment [6]. At the current configuration a CE value of 0.4% in-band EUV in 2π has been reached. Investigation of the physical properties of the source as well as of the performance of the source from the lithographic point of view is in progress.

Besides the evaluations being done at ASML, we are investigating EUV discharge sources with alternative target material with ISAN, in Troitsk, Russia. Alternative target materials being investigated include Li, Sn, and In. [3]. It is generally expected that production tool sources will require a non-Xe target material in order to achieve the necessary power to support high tool throughput. Compared to Xe-based sources that have a typical conversion efficiency around 0.5%, the investigated materials Sn and In were found to have a CE of 2% and 1%, respectively. Examples of spectra that have been measured for the various materials are plotted in Figure 4. Further understanding of the physical processes of the source as well as engineering improvements is needed in order to fulfill the EUV lithography roadmap.

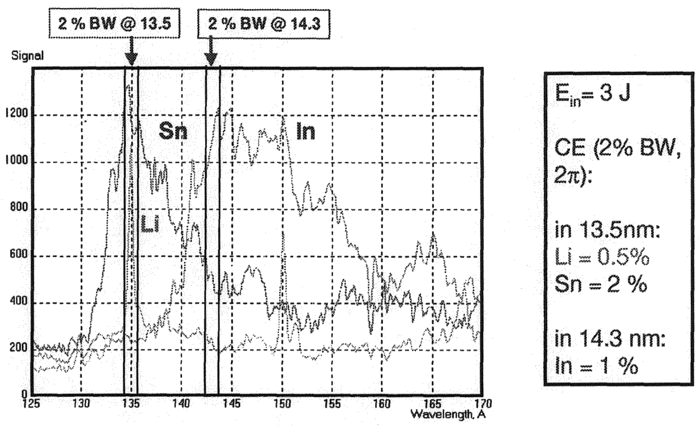

Figure 4. Emission spectra of experimental non-Xe discharge sources [3].

2.2. System design

Last year we reported on the general vacuum design of the α-tool [4]. We described that the α-tool is divided into 5 separate vacuum compartments: source chamber, main chamber, wafer stage chamber, wafer handling module, and reticle handling module. The main chamber contains both the illumination- and projection optics as well as the reticle stage and the metrology frame. The partial pressure of H_2O in the main chamber is specified at 10^{-7} mbar, and the hydrocarbon (C_XH_Y) pressure at 10^{-9} mbar. A detailed vacuum budget has been specified, allocating fractions of the total outgassing rates for H_2O and C_XH_Y to the modules that comprise this main chamber, including the baseframe wall, metrology frame surface, cables, hoses, motors, projection optics, reticle stage interferometry, etc. The wafer stage compartment includes the alignment- and focus sensors and wafer stage interferometry, and has a less stringent vacuum specification than the main chamber: 10^{-5} mbar for H_2O and 10^{-7} mbar for hydrocarbons. Both chambers are separated by a gas lock that uses a downward gas flow to prevent outgassing resist molecules from reaching the optics.

We recently completed the vacuum qualification of the focus sensor. Its outgassing rates were found to be within the specifications: 8.6×10^{-5} mbar·l/s for H_2O (spec: 1.9×10^{-4} mbar·l/s), and 5.4×10^{-8} mbar·l/s for C_XH_Y (spec: 2.2×10^{-7} mbar·l/s). These outgassing rates were achieved by carefully selecting fibers, cables, glues, and material for the mechanical structure, as well as through smart 'vacuum-compliant' design approaches including elimination of dead volumes, drilled-through holes, etc.

Six degree of freedom position information of the reticle and wafer in the lithography tool is obtained through an interferometric measurement system. These wafer- and reticle stage measurement systems are mounted to a super-Invar metrology frame, as are the projection optics and alignment- and focus sensors. The metroframe is located in the main chamber and therefore contributes to its vacuum performance; proper material choice, good surface finish, and minimizing its surface area therefore are crucial to meet the vacuum budget. In Figure 5 several stages of its manufacturing process are visualised.

Figure 5. Manufacturing of the wafer metrology sensor frame. On the left the raw material for the bottom part, on the right the machining of the top part of the frame.

2.3. Wafer- and reticle stage scan performance

The motion system of the α-tool consists of a wafer stage and a reticle stage. Both stages are based on a dual-actuator configuration, where the coarse motion is provided by a long stroke actuator and the fine motion by a short stroke actuator. The short strokes are driven using contactless Lorentz actuators. Measurements of the reticle and wafer stage position in 6 degrees of freedom (DOF) are done by means of a laser interferometer measurement (IFM) system with sub-nanometer resolution. This IFM system is mounted on the metrology frame which is weakly suspended on the ground using air mounts. The wafer- and reticle stages are actively controlled in 6 DOF's at control bandwidths ≥ 100 Hz.

The α-tool stages have been tested as two separate and independent test rigs. At present they operate in air, which enables easy access for development and reduces downtime since we do not have to evacuate the compartment. Until recently aluminum short stroke stages were used, with small mirrors attached to the sides to enable the use of the IFM system. As a consequence, only small scans around the center position of the stage could be made. At present, experiments are ongoing with Zerodur short stroke stages, where the performance of the stages over the entire 300-mm stroke can be assessed.

In the left-hand side of Figure 6 the first scanning performance of the wafer stage in y-direction is shown, after limited servo tuning. A scan of length 3 cm was made in the y direction at a constant scanning velocity of 0.1 m/s and a maximum acceleration of 2 m/s^2. The moving average MA and moving standard deviation MSD of the position error in y-direction are computed assuming a slit width of 2 mm. It can be seen that the peak value of the MA–which occurs during acceleration and deceleration–is about 7 nm. The peak MSD value is about 12 nm, again during acceleration and deceleration. In the actual 'exposure' scanning-interval where the velocity is constant–from approximately 0.06 s to 0.28 s–the MA is in the order of 1 nm, whereas the MSD does not exceed 7 nm. This level of performance is sufficient to support sub-50nm imaging, and we are currently investigating achieving this performance at higher scan velocities. Although the current air test rig has been made fully compatible with its vacuum counterpart, testing on the final vacuum module is required in order to verify that the same performance can be achieved under vacuum conditions.

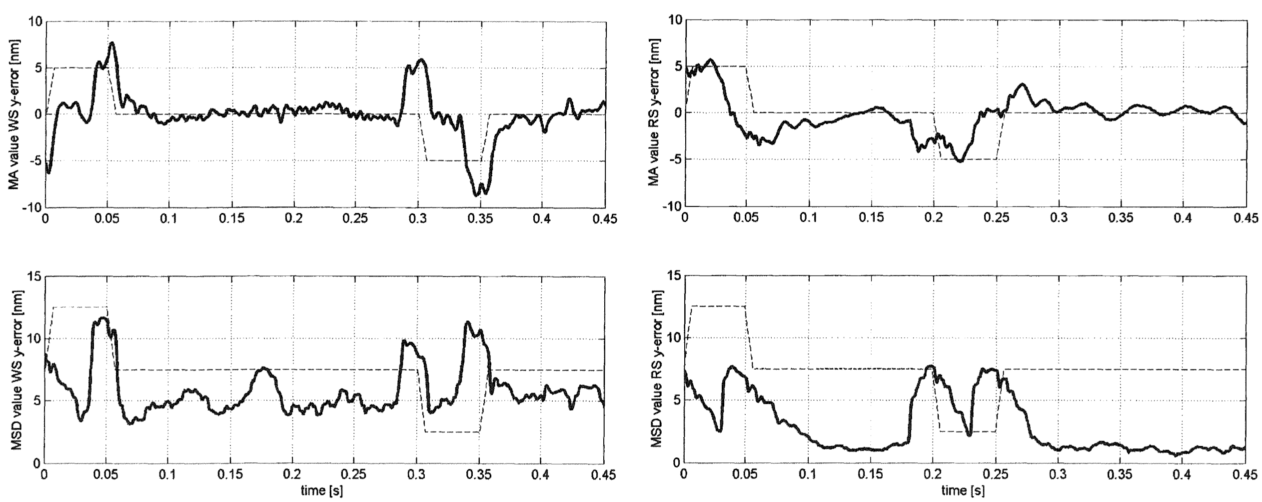

Figure 6. Positioning accuracy of the α-tool wafer stage (left) and reticle stage (right). Top-row images show the calculated moving average MA as a function of time, the bottom-row images the moving standard deviation MSD. The dotted lines in the top figures represent the acceleration profile.

On the right-hand side of Figure 6 the scanning performance of the reticle stage in y-direction is shown. A scan of length 8 cm was made in the y-direction at a scanning velocity of 0.4 m/s and a maximum acceleration of 8 m/s^2. The MA and MSD values of the position error are again computed assuming a slit width of 2 mm at wafer level. The peak of the MA during acceleration and deceleration is about 6 nm. The peak MSD value is approximately 8 nm, also during acceleration and deceleration. In the actual scanning-interval, from approximately 0.06 s to 0.18 s, the MA is in the order of 2 nm, whereas the MSD does not exceed 5 nm. As with the wafer stage, this level of performance for the reticle stage is good enough to support sub-50nm imaging at low throughput, and preliminary reticle stage tests at higher scan velocities show that the accuracy requirements can be maintained.

2.4. Wafer handler

The α-tool wafer handling module consists of an atmospheric front-end and a vacuum back-end. The front-end includes a FOUP and prealignment unit, and interfaces with a track system. Use of the atmospheric front-end of the TWINSCAN™ illustrates re-use of existing ASML technology to ensure that focus is kept on the new vacuum specific issues where necessary. The custom-made vacuum back-end interfaces with the main body of the system and contains the wafer loadlock chambers and a robot for wafer transfer. We selected a single-wafer loadlock approach for the α-tool, which is sufficient to achieve the required throughput of ≥1 wph.

In 2001 a test setup was built to measure pumpdown behaviour of the loadlock chamber, particularly the thermal behaviour of the wafer. In 2002 we extended the experiments to include fast and slow pumping strategies, to study minimization of particle generation and temperature gradients.

The wafer handling functional model–which can demonstrate the wafer takeover process flow to a simplified dummy wafer stage–is in the realisation phase: we expect the module to be functional in the Summer of this year. A photograph of the setup can be seen in Figure 7. The complete vacuum wafer handler that will be integrated in the α-tool will be finished at the end of the year.

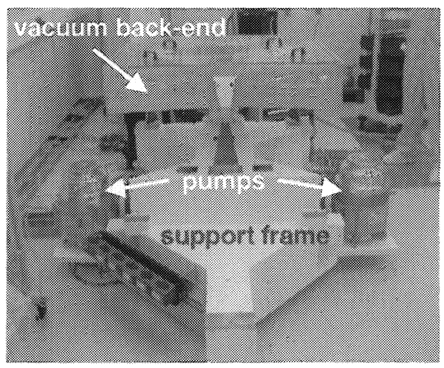

Figure 7. Wafer handling functional model. The vacuum pumps, the atmospheric front-end (not yet installed), and the vacuum back-end are all mounted on a common support frame.

3. PARTICLE DETECTION AND STANDARDISATION IN RETICLE HANDLING

3.1. Particle detection

EUV reticles can not have a protecting pellicle, since no material with adequate thickness is known that can transmit EUV radiation. Keeping the mask free of particles ≥ 50 nm both at the front and the backside during all handling steps in the life of a pellicle-less reticle is a major challenge. ASML has launched a particle contamination control program at TNO TPD in Delft in order to gain knowledge and experience in this field. Experiments have been performed to investigate the most important aspects of particle contamination during the life of a mask. The possible sources of particles, the migration aspects, and the influence of vacuum and atmospheric pressures have been investigated, and experimental results have been reported earlier [4].

Part of the particle control program is to qualify the α-tool reticle handler module, which includes a storage container, vacuum loadlock, and transfer mechanism into the scanner. Qualifying includes scanning reticle blanks for added particles, where the blanks are handled many times through the system. For this purpose a dedicated surface scanner was developed and built, see Figure 8. First results show that particles below 50 nm can be observed. The goal is to scan surfaces having the same dimensions and topology as an EUV mask pattern, to allow us to identify solutions to cross-contamination during the handling experiments. Full-size experiments using the prototype reticle handler and storage container are planned. The substrates that will be used are EUV blanks without pattern. The optical scattering technology and software is currently being improved to reduce the scanning time from several days to several hours, in order to be more compliant with the production environments and serial qualification runs.

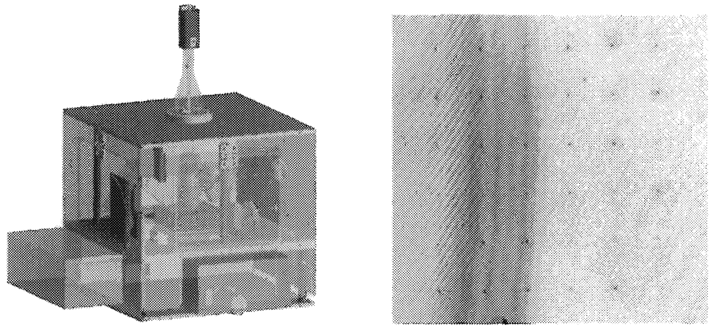

Figure 8. Particle detection system for reticle handling qualification (left) and first results where a matrix of intentionally etched 50nm structures can be distinguished (right).

3.2. Reticle storage, gripping, and handling standardisation

ASML has stimulated the development SEMI Standards for EUV reticle handling and storage. Contamination control (both particulate and molecular) requirements are more stringent as compared to DUV lithography due to the issues mentioned in the previous section. In addition, overlay specifications for EUV are much tighter than for DUV ($\leq$ 15nm), with the result that errors due to reticle clamping must be driven even lower (2.5 nm for the litho tool and 2 nm for the e-beam writing tool) due to the non-telecentric illumination of the reticle. This leaves very little for all the other overlay contributors, including front side and back side flatness, and pattern placement errors.

ASML's current efforts include collaborating with SEMI to refine the draft standard 3419 on EUV Mask Chucking, originally proposed by ASML as the "Three Rule Standard". Rather than specify chuck design or type, ASML reduced clamping to three rules. They are clamping pressure, clamp stiffness and clamp flatness. If met, they ensure that clamps used to hold EUV reticles during critical steps in the manufacturing and usage do not introduce different in-plane or out-of-plane distortion, reducing overlay errors. The critical steps are pattern generation in e-beam writing tools, inspection in mask shops, and exposure during scanning in the lithography tool.

Recognizing the strict contamination control requirements for the lithography tool and the masks used in them, we realized that without providing a clean, contamination-free storage and transport environment, EUV masks would never produce usable wafers. ASML began working on concepts for storage and handling of masks and shared these ideas with other members of the mask infrastructure via the SEMI standards committees and the newly formed Reticle Protection Working Group. The objective is to develop a standard for mask storage by defining a storage box that could be used in all steps of mask handling – throughout the mask shop, transport to Litho tool suppliers, and movement within customer fabs. Figure 9 below shows a concept that we have developed for the mask storage box.

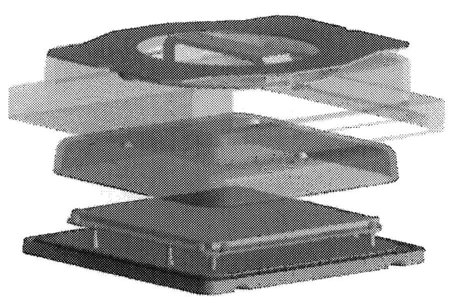

Figure 9. Exploded view of a proposed standard EUV reticle storage box.

4. OPTICS DEVELOPMENT

Within ASML's EUV program Carl Zeiss SMT AG is responsible for the development of the optical train, comprising an illuminator and a six mirror projection optics box, PO Box. The design phase of the optical train was finished some time ago. We now have started the fabrication of components of the optical train of the α-tool.

In this phase of the program the main challenges are:

- meeting the lifetime requirements for the α-tool and future tools for process development and production,
- the fabrication of the aspheric mirrors of the PO Box,
- the fabrication of special components (collector, integrator) in the illuminator,
- meeting the mechanical stability requirements of the PO Box mirrors: during wafer exposure the PO Box mirrors have to be stabilized with sub nm, sub nrad accuracy,
- setting up the system metrology for alignment and qualification of the optical train.

Here, we focus on the status of illuminator development and optics fabrication, and give a short overview of our lifetime program.

4.1. Illuminator

Although we have selected the hollow-cathode-triggered (HCT) discharge source for the α-tool it is not yet clear which source type will eventually be chosen for later EUV process development and production tools. Thus, we have developed a flexible design solution which can be adapted to different source types. With this modular approach "only" the collector design has to be optimised for different sources while the rest of the illuminator stays essentially the same, see Figure 10.

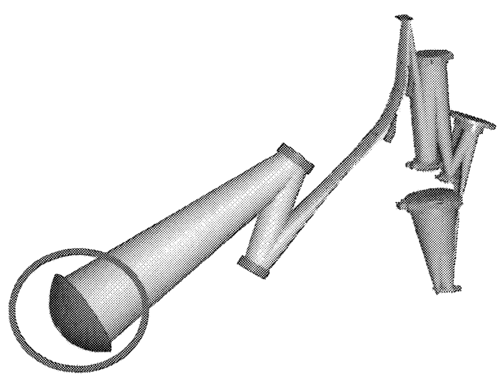

Figure 10. Schematic overview of a typical illuminator and PO Box design. For different source types the collector unit (red circle) has to be modified.

Discharge sources are generally rather large (typical plasma dimensions: diameter = 1.3 mm, length = 1.6 mm) which means that the collection angle is relatively small. A possible design option is the use of a nested grazing incidence collector consisting of several densely packed concentric mirror shells. LPP sources on the other hand tend to be smaller: a plasma diameter smaller than 100 µm is possible, which means that normal incidence collectors covering a larger collection angle might be used (example of Figure 10) [7].

A second important design rule–besides the choice of a modular concept for the collector/illuminator unit–was that the design had to be optimized for the manufacturability of its components. To verify the manufacturability of potential design solutions, we have fabricated demonstrator elements of integrator mirrors, spectral purity filters, and different types of collectors. Examples of such demonstrator elements are given in Figure 11 where an individual collector shell is shown.

Figure 11. Individual shell for a grazing incidence collector.

4.2. Optics fabrication

The fabrication of the off-axis mirrors of the PO Box is one of the main challenges for EUV. We have reported on the status of our fabrication technology previously [4]. As has been pointed out earlier, we develop our fabrication technology by manufacturing Micro Exposure Tool (MET) mirrors. The two-mirror MET PO Box was developed in a joint project of Lawrence Livermore National Labs and Zeiss. The first two PO Boxes were fabricated within the scope of this project. Meanwhile, at Zeiss we have developed also an illuminator. The complete optical train, consisting of the PO Box and the illuminator will this year be integrated into a commercial EUV stepper.

MET mirrors are on-axis mirrors and they are smaller than the off-axis mirrors of the typical six-mirror system that is used in an EUV production tool. Also, mirror asphericities and the gradients of the asphericity on MET mirrors are smaller than on the most critical off-axis mirrors [4]. Thus, MET mirrors are good candidates for the development of new fabrication strategies. In the next phase, the MET fabrication strategies are applied to the fabrication of off-axis aspheres. At Zeiss, production of a first set of α-tool off-axis aspheres has started, and first results are expected within the next months.

Here, we report on the status of our MET mirrors. The quality of these mirrors is characterized by the power spectral density (PSD). The PSD is divided into three ranges, the figure, the mid spatial frequency roughness (MSFR), and the high spatial frequency roughness (HSFR). The MSFR includes all frequencies that contribute to in-field scattering and determines the flare and thus the contrast of the optical system. Therefore, reducing the MSFR level is one of the main goals of optics fabrication technology. Table 1 shows that substantial progress has been made in optimizing the MSFR, and also in obtaining better figure and HSFR values. Set 3 demonstrates our current optics fabrication capability.

Table 1. Status of the mirror fabrication technology.

Mirror M2 (MET)			
	SET 1	SET 2	SET 3
Figure: ≥ 1 mm	0.25 nm rms	0.21 nm rms	0.20 nm rms
MSFR: 1 mm – 1 μm	0.34 nm rms	0.28 nm rms	0.20 nm rms
HSFR: ≤ 1 μm	0.38 nm rms	0.31 nm rms	0.20 nm rms

Going from the MET to a full-field six mirror system we have larger mirrors and a substantially larger field (26 x 2 mm for the α-tool, compared to 0.2 x 0.6 mm for the MET). This means that light scattered into a wider angle reaches the imaging field and thus an extended MSFR range is contributing to the flare of the α-tool system. The MSFR of a six-mirror system includes 4.7 decades of the PSD compared to roughly 3 decades for a MET mirrror. If the PSD of M2/Set 3 is evaluated for the larger six mirror system range this results in an rms value of 0.27 nm. For production tools, a flare level less than 10% is required, corresponding to a MSFR level smaller than 0.15 nm rms. Developing volume production processes for the fabrication of systems with such a low flare level will be a major challenge for EUV optics fabrication.

4.3. Contamination Control

We have set the lifetime target for EUV optical systems to 30,000 hours of exposures. Our lifetime definition is as follows: the system is out of specification, if an irreversible reflectivity loss of more than 1% per mirror occurs. This corresponds to a transmission loss of ~10% in the overall system. The environment control effort therefore is driven by these lifetime requirements, since mirror reflectivity degradation due to EUV induced oxidation or carbon growth is one of the main contributors to optics lifetime. In comparison, the Engineering Test Stand ETS has up to now been operational for several hundreds of exposure hours, however at a much lower EUV power level of typically ~0.3 W in-band EUV collected [9] than the power levels that are foreseen for production tools ($\geq$ 115 W), and even in the α-tool (5–15 W).

Oxidation is irreversible–to our knowledge no recovery procedure has been identified–and must therefore be prevented at all times. At the partial pressures for the α-tool as specified in Section 2.2 of 10^{-9} mbar C_XH_Y and 10^{-7} mbar H_2O we expect carbon growth to be the dominant degradation mechanism, and therefore a cleaning- or mitigation strategy must be developed. A periodic cleaning of the system as shown in the diagram in Figure 12 might be possible, and several groups have demonstrated methods for cleaning a mirror surface [10,11].

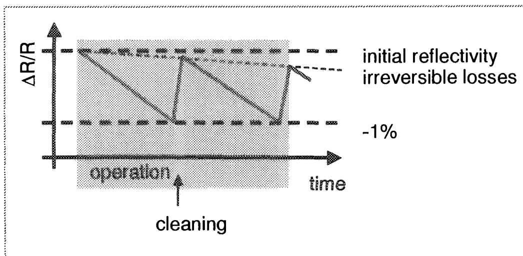

Figure 12. Periodic cleaning can (partially) restore the reflectivity of a C-contaminated mirror surface. The mirror is out of specification when irreversible contamination and/or damage of the mirror coating caused by the cleaning process, results in a reflectivity loss of more than 1%.

In Figure 13a we show the reflectivity plot of a bare MoSi sample exposed for 8h to an EUV intensity of 5 mW/mm^2 at a H_2O partial pressure of 10^{-6} mbar. Note that this is a 10× higher pressure than specified for the α-tool. It can be seen that the reflectivity is reduced by 4%, leading to a reflectivity loss rate of 0.5%/h. Auger depth profiling shows that the reflectivity loss is caused by oxidation, therefore the MoSi lifetime under these conditions is only 2h. Potential solutions to increase lifetime of the optical train of an EUV system include

- increasing the oxidation resistance of the coating. A strategy that has been proposed is the application of a cap layer on top of the multilayer coating. Materials that are suggested include Ru [12] and C [13].
- Implementing "softer" cleaning strategies that don't damage the multilayer stack.
- Improving the vacuum conditions in the system: at present the hydrocarbon partial pressure in the optics compartment is specified at 10^{-9} mbar, whereas the H_2O partial pressure is specified at 10^{-7} mbar. An order of magnitude reduction of these pressures increases lifetime roughly one order of magnitude, but might complicate the mechanical design of lithography systems to an unacceptably high level.
- Implementing carbon growth mitigation strategies, using *e.g.* reactive O_2 during exposure [10].
- A combination of the above.

Using caplayers a significant improvement in the oxidation resistance is observed. In Figure 13b a capped sample was exposed under similar conditions as the uncapped sample, but now for 50h. The reflectivity loss was found to be 0.28% ± 0.15%, which translates to a reflectivity loss rate of ~5×10^{-3} %/h. This is a 100× improvement over the uncapped sample.

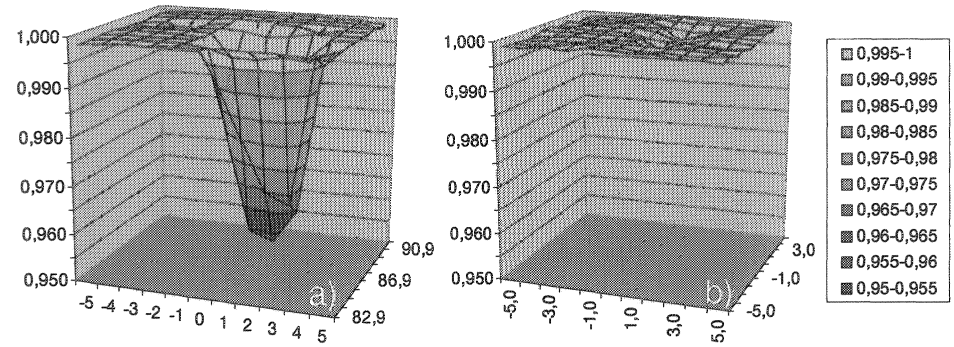

Figure 13. a) reflectivity degradation of a 8h exposed bare MoSi sample, and b) a 50h exposed capped MoSi sample. An improvement $\geq 100\times$ in oxidation resistance is observed. For a description of the experimental conditions, see text.

Although the results so far show significant progress, still several orders of magnitude improvement are required, and thus increasing the lifetime of the optical train is one of the focal points of our EUV program. In the past year, at Zeiss and its partner laboratories the infrastructure for implementing and testing contamination control strategies has been set up. Most notable are the completion of a large reflectometer at the radiometrology laboratory of the PTB at BESSY 2 in Berlin and the start of experiments at our in-situ reflectometer at a beam line dedicated to contamination experiments, also at the PTB laboratory. The description of both setups and first experimental results will be published separately at this conference [14,15].

5. CONCLUSIONS

The α-tool project is in the realisation phase of most of the modules. The alignment- and focus sensor are assembled, and the focus sensor was found to meet the vacuum outgassing rate specifications. Both the wafer- and reticle stage for the α-tool are operational, and preliminary scanning performance in the air setups has given us great confidence that the performance specifications lateron in vacuum will be met. Automated wafer- and reticle handling modules are being realised. Preliminary data shows that a in-house newly developed particle scanner is able to detect 50nm particles. Polishing for the Set 3 MET secondary optics has met the figuring and MSFR requirements. Technology transfer to the α-tool optical elements is now in progress. Using caplayers on top of MoSi multilayer mirror samples has demonstrated an oxidation rate suppression of $\geq 100\times$, as compared to bare MoSi samples.

ACKNOWLEDGEMENTS

The authors would like to emphasize that the work presented here has been a team effort, with contributions by a large number of people in various organizations. The following are gratefully acknowledged for their contributions: Philips, TNO TPD, FOM Rijnhuizen, PTB-BESSY, and Lawrence Livermore and Lawrence Berkeley National Labs. The work at ASML has partly been sponsored by the Dutch Ministery of Economic Affairs, and the work at Zeiss has been supported by the Bundesministerium für Bildung und Forschung (Project 13N8088). The MET work was partially funded by International SEMATECH Project Lith-112.

REFERENCES

1. H. Meiling, J.P.H. Benschop, U. Dinger, and P. Kürz, "Progress of the EUVL alpha tool", *SPIE Symposium on Emerging Lithographic Technologies V*, Vol. 4343, p. 38 (2001).
2. See various authors at 1st International EUV Lithography Symposium, Dallas, TX, USA (2002), and various authors in *SPIE Symposium on Emerging Lithographic Technologies VI*, Vol. 4688 (2002).
3. V. Banine, H. Franken, R. Gontin, and R. Moors, "Requirements for Next Generation Lithography EUV sources", 1st International EUV Lithography Symposium, Dallas, TX, USA (2002).
4. H. Meiling, J.P.H. Benschop, R. Hartman, P. Kürz, P. Høghøj, R. Geyl, and N. Harned, "EXTATIC, ASML's α-tool development for EUVL", *SPIE Symposium on Emerging Lithographic Technologies VI*, Vol. 4688, p. 52 (2002).
5. K. Bergman *et al.*, Appl Opt. 39 (2000) 3833-3837.

6. R. Stuik, H. Fledderus, P. Hegeman, J. Jonkers, M. Visser, V Banine, and F. Bijkerk, "Flying Circus EUV source comparison, absolute yield, absolute yield fluctuations and contamination", Second SEMATECH Workshop on Extreme UV Lithography, San Francisco, USA (2001).
7. M. Antoni, W. Singer, J. Schultz, J. Wangler, I. Escudero-Sanz, and B. Kruizinga, "Illumination Optics Design for EUV-Lithography," *SPIE Symposium on Optical Science and Technology,* Vol. 4146, p. 25 (2000).
8. P. Kürz *et al.*, "Optics for EUV Lithography", 1st International EUV Lithography Symposium, Dallas, TX, USA (2002).
9. W. P. Ballard, L. J. Bernardez, R. E. Lafon, R. J. Anderson, H. Shields, M. B. Petach, and R. J. St. Pierre, "High-Power Laser-Produced-Plasma EUV Source," *SPIE Symposium on Emerging Lithographic Technologies VI*, Vol. 4688, p. 302 (2002).
10. S. Graham, M.E. Malinowski, C.E. Steinhaus, P.A. Grunow, and L.E. Klebanoff, "Studies of EUV contamination mitigation", *SPIE Symposium on Emerging Lithographic Technologies VI*, Vol. 4688, p. 431 (2002).
11. M. Malinowski, C. Steinhaus, M. Clift, L.E. Klebanoff, S. Mrowka, and R. Soufli, "Controlling contamination in Mo/Si multilayer mirrors by Si surface-capping modifications", *SPIE Symposium on Emerging Lithographic Technologies VI*, Vol. 4688, p. 442 (2002).
12. L. Klebanoff, S.J. Haney, P.A. Grunow, W.M. Clift, and A.H. Leung, "Rates of Optics contamination in the Engineering Test Stand (ETS)", 1st International EUV Lithography Symposium, Dallas, TX, USA (2002).
13. H. Meiling, R. Hartman, R. Moors, M. Renkens, H. Werij, and P. Kürz, "Update on the EUV Lithography alpha tool", 1st International EUV Lithography Symposium, Dallas, TX, USA (2002).
14. Bas Mertens *et al.*, this conference.
15. G. Ulm *et al.*, this conference.